

## Failure to Insert the Iron-Sulfur Cluster into the Rieske Iron-Sulfur Protein Impairs Both Center N and Center P of the Cytochrome $bc_1$ Complex\*

Received for publication, August 21, 2002, and in revised form, October 7, 2002  
Published, JBC Papers in Press, October 10, 2002, DOI 10.1074/jbc.M208556200

Emma Berta Gutierrez-Cirlos, Torsten Merbitz-Zahradnik, and Bernard L. Trumpower‡

From the Department of Biochemistry, Dartmouth Medical School, Hanover, New Hampshire 03755

**Mutation of a serine that forms a hydrogen bond to the iron-sulfur cluster of the Rieske iron-sulfur protein to a cysteine results in a respiratory-deficient yeast strain due to formation of iron-sulfur protein lacking the iron-sulfur cluster. The Rieske apoprotein lacking the iron-sulfur cluster is inserted into both monomers of the dimeric cytochrome  $bc_1$  complex and processed to mature size, but the protein lacking iron-sulfur cluster is more susceptible to proteolysis. In addition, the protein environment of center P in one half of the dimer is affected by failure to insert the iron-sulfur cluster as indicated by the fact that only one molecule of myxothiazol can be bound to the cytochrome  $bc_1$  dimer. Although the  $bc_1$  complex lacking the Rieske iron-sulfur cluster cannot oxidize ubiquinol through center P, rates of reduction of cytochrome  $b$  by menaquinol through center N are normal. However, less cytochrome  $b$  is reduced through center N, and only one molecule of antimycin can be bound at center N in the  $bc_1$  dimer lacking iron-sulfur cluster. These results indicate that failure to insert the [2Fe-2S] cluster impairs assembly of the Rieske protein into the  $bc_1$  complex and that this interferes with proper assembly of both center P and center N in one half of the dimeric enzyme.**

The Rieske iron-sulfur protein is an essential subunit of mitochondrial cytochrome  $bc_1$  complexes that is encoded by a nuclear gene, synthesized on cytoplasmic ribosomes, and then imported into the mitochondria and assembled into the cytochrome  $bc_1$  complex in the inner mitochondrial membrane (1). During import and assembly into the  $bc_1$  complex a presequence is cleaved from the iron-sulfur protein precursor, and a [2Fe-2S] cluster is inserted into the protein. In *Neurospora crassa* and *Saccharomyces cerevisiae* the presequence is removed in two steps, whereas in mammals the presequence is cleaved in a single step and retained as a subunit in the  $bc_1$  complex (2). In *Schizosaccharomyces pombe* processing of the iron-sulfur protein precursor also occurs in one step but can be converted to two step processing by changing a proline in the presequence to a serine (3). The two step processing of the iron-sulfur protein precursor that occurs in *S. cerevisiae* is not essential for import and assembly of functionally active iron-sulfur protein into the  $bc_1$  complex because mutated forms of

the iron-sulfur protein that are processed to mature size in a single step are properly assembled into the  $bc_1$  complex and are functional (4).

We previously investigated the relationship between assembly of the apoprotein into the  $bc_1$  complex and insertion of the [2Fe-2S] cluster in *S. cerevisiae*. We showed that the apoprotein can be assembled into the  $bc_1$  complex if the cluster is not inserted (5), which suggests that the [2Fe-2S] cluster is added after the apoprotein is assembled into the  $bc_1$  complex. We also showed that if processing of intermediate to mature size iron-sulfur protein is blocked by mutations in the presequence, the intermediate size iron-sulfur protein accumulates in the  $bc_1$  complex and is functionally active (6). This result establishes that the second protease-processing step takes place after intermediate size iron-sulfur protein has been assembled into the  $bc_1$  complex and that the [2Fe-2S] cluster is inserted into the apoprotein before the second protease-processing step, although it does not establish that this sequence of events is obligatory.

We have now characterized the cytochrome  $bc_1$  complex from a yeast mutant in which the [2Fe-2S] cluster is not inserted into the Rieske iron-sulfur protein due to a mutation of a serine that forms a hydrogen bond to the iron-sulfur cluster to a cysteine. We show that although the protein lacking the iron-sulfur cluster is assembled into the  $bc_1$  complex and processed to mature size, it is structurally abnormal, as evidenced by susceptibility to protease degradation. In addition, failure to insert the [2Fe-2S] cluster impairs both center P and center N. These results are discussed in relation to how insertion of the iron-sulfur cluster affects assembly of the Rieske protein into the  $bc_1$  complex and the structure of the  $bc_1$  dimer.

### EXPERIMENTAL PROCEDURES

**Materials**—Dodecylmaltoside was obtained from Roche Molecular Biochemicals. DEAE-Biogel and ammonium persulfate were obtained from Bio-Rad Laboratories. Acrylamide and bis-acrylamide were from National Diagnostics. TEMED<sup>1</sup> was from Invitrogen. Yeast extract and peptone were from Difco. Nitrogen Base without amino acids but with ammonium sulfate was from US Biological. Antimycin, DFP, phenylmethylsulfonyl fluoride, menaquinone, and dithionite were purchased from Sigma. Stigmatellin was purchased from Fluka Biochemica.

**Purification of  $bc_1$  Complexes**—Yeast cytochrome  $bc_1$  complexes were isolated as described previously (7, 8). The CHS14 yeast mutant was obtained by site-directed mutagenesis as described by Denke *et al.* (9). The wild-type yeast strain, W303-1A, was grown in 1% yeast extract, 2% peptone, and 2% dextrose medium and harvested by centrifugation. The CHS14 yeast mutant was grown in a defined medium containing 2% dextrose, 0.7% of nitrogen base without amino acids but with ammonium sulfate, and 0.15% of amino acid supplement minus tryptophan.

\* This work was supported by National Institutes of Health Research Grant GM20379. The costs of publication of this article were defrayed in part by the payment of page charges. This article must therefore be hereby marked "advertisement" in accordance with 18 U.S.C. Section 1734 solely to indicate this fact.

‡ To whom correspondence should be addressed: Dept. of Biochemistry, Dartmouth Medical School, 7200 Vail, Hanover, NH 03755. Tel.: 603-650-1621; Fax: 603-650-1389; E-mail: Trumpower@Dartmouth.edu.

<sup>1</sup> The abbreviations used are: TEMED, *N,N,N',N'*-tetramethylethylenediamine; DFP, diisopropylfluorophosphate; OTTLE, optically transparent thin layer electrode; CD, circular dichroism; NHE, normal hydrogen electrode; CPK, Corey, Pauling, Kuntz.

**Circular Dichroism Spectra of Purified Cytochrome  $bc_1$  Complexes**—The  $bc_1$  complexes were concentrated by ultracentrifugation as isolated at pH 7.0. Mediators were added to facilitate redox equilibration, and potentiometric titrations were monitored by CD spectroscopy using an OTTLE cell as described previously (9, 10). The concentrations of the  $bc_1$  complexes and the path-length of the OTTLE cell were 845  $\mu\text{M}$  and 40  $\mu\text{m}$ , respectively, for the enzyme from the wild-type yeast, and 430  $\mu\text{M}$  and 100  $\mu\text{m}$  for the enzyme from the CHS14 mutant. CD spectra were recorded at 4 °C and a scan rate of 200 nm/min, accumulating four scans per spectrum. The fully reduced spectra were taken at  $-413$  mV (wild-type) and  $-411$  mV (CHS14), and the fully oxidized spectra were taken at  $+487$  mV (wild-type) and  $+489$  mV (CHS14). The spectra were taken after complete equilibration to the applied potentials, which are given relative to NHE.

**Western Analysis of Mitochondrial Membranes and  $bc_1$  Complexes**—Mitochondrial membranes and purified  $bc_1$  complexes from W303 and CHS14 cells were resolved in 15% SDS-PAGE gels (11). The gels were stained with Coomassie Blue or blotted to nitrocellulose membranes. Iron-sulfur protein and cytochrome  $c_1$  were detected by Western blotting (12) using monoclonal antibodies to the yeast proteins (5). The stained gels were scanned, and the intensities of the signal were quantified using a UMAX scanner and the NIH Image software.

**Determination of Inhibitor Concentrations**—Each of the inhibitors was diluted in ethanol, and the concentration was determined from optical spectra obtained in an Aminco DW2a™ UV/Visible spectrophotometer with the OLIS DW2 conversion and OLIS software. The difference spectrum, after subtracting the ethanol background, was recorded from 250–400 nm. To accurately determine the concentration for each inhibitor, the absorbance was measured at concentrations that yielded 0.1–0.15 absorbance units after diluting stock solutions of the inhibitors. To minimize random dilution errors, each dilution was performed 5 or 6 times, and the diluted solutions were combined. The extinction coefficients used to calculate the concentrations of the stock solutions were, for antimycin,  $4.8 \text{ mM}^{-1}\text{cm}^{-1}$  at 320 nm, for stigmatellin,  $65.5 \text{ mM}^{-1}\text{cm}^{-1}$  at 267 nm, and for myxothiazol,  $10.5 \text{ mM}^{-1}\text{cm}^{-1}$  at 313 nm (13). All of the inhibitor dilutions were prepared daily, and the concentrations were determined before a titration was started.

**Pre-steady State Reduction of Cytochrome  $b$** —Pre-steady state reduction of cytochrome  $b$  was followed at room temperature by stopped flow rapid scanning spectroscopy using the OLIS Rapid Scanning Monochromator (On-Line Instrument Systems, Inc., Bogart, GA). The spectrophotometer was equipped with a 1200 lines/nm grating blazed at 500 nm. This produced a 75-nm spectrum, centered at 550 nm, with a resolution of 0.4 nm. The dead time of the instrument was 2 ms, and the end of this period was chosen as time zero. Data was collected at 1000 scans/s. The rationale for this pre-steady state kinetics method was discussed previously (14).

Reactions were started by rapid mixing of 3  $\mu\text{M}$   $bc_1$  complex in assay buffer containing 50 mM potassium phosphate, pH 6.0, 250 mM sucrose, 1 mM sodium azide, 0.2 mM EDTA, and 0.01% Tween 20 against an equal volume of the same buffer containing 50  $\mu\text{M}$  menaquinol. A fresh solution of menaquinol substrate was prepared from menaquinone before each experiment as described previously (8). The  $bc_1$  complex was diluted shortly before each titration. The exact  $bc_1$  concentration was determined by difference spectra recorded in the Aminco DW2a™ spectrophotometer. The cytochrome  $c_1$  concentration was determined from the difference spectrum of the ascorbate-reduced versus ferricyanide-oxidized enzyme, using an extinction coefficient of  $17.5 \text{ mM}^{-1}\text{cm}^{-1}$  at 553–548 nm (15). Cytochrome  $b$  concentration was determined from the difference spectrum of the dithionite-reduced versus ferricyanide-oxidized enzyme, using an extinction coefficient of  $25 \text{ mM}^{-1}\text{cm}^{-1}$  at 563–578 nm (15). To determine the rate constants for reduction of cytochrome  $b$  through center N, the  $bc_1$  complex from the wild-type yeast was mixed with a 2-fold excess of stigmatellin to block the reaction through center P. It was not necessary to include stigmatellin with the  $bc_1$  complex from the CHS14 mutant because the absence of iron-sulfur cluster prevents reduction of cytochrome  $b$  through center P.

To determine the titer for inhibition of the reduction of cytochrome  $b$  with antimycin, the antimycin was incubated with the enzyme 2 min before starting the reaction. An oxidized spectrum was obtained by mixing the oxidized  $bc_1$  complex against assay buffer and averaging the data sets to a single scan. For each inhibitor concentration, three data sets were averaged, and the oxidized spectrum was subtracted from each scan. From the three-dimensional data set comprised of wavelength, absorbance, and time, the time course and amplitude change for cytochrome  $b$  reduction at 563 nm was extracted using the OLIS software.

**Measurement of the Red Shift in the Cytochrome  $b$  Spectrum**—The  $bc_1$  complex was diluted to an approximate concentration of 3  $\mu\text{M}$  in

assay buffer (pH 7.0), and the exact concentration was determined as described above. A baseline was obtained by reducing the  $bc_1$  complex with dithionite in both sample and reference cuvettes in the Aminco DW2a™ spectrophotometer. Increasing amounts of antimycin were added to the sample cuvette and an equal amount of ethanol to the reference cuvette. After allowing the inhibitor to equilibrate with the enzyme for 2 min, a difference spectrum was recorded for each concentration of inhibitor added. For each inhibitor concentration the absorbance difference at 565–558 nm was determined. The same procedure was used to measure the red shift induced by myxothiazol binding, except the absorbance difference at 564–559 nm was determined.

**Quenching of Antimycin Fluorescence by the  $bc_1$  Complex**—Binding of antimycin to the wild-type and CHS14 mutant  $bc_1$  complexes was measured by the quenching of antimycin fluorescence. The method was essentially as described by Berden and Slater (16). Briefly, a sample of W303 or CHS14  $bc_1$  complex was diluted to an approximate concentration of 2  $\mu\text{M}$  in assay buffer at pH 7.0, and the exact concentration was determined in the Aminco DW2a™ spectrophotometer as described above. Antimycin fluorescence was measured with a Hitachi fluorescence spectrophotometer model F-3010 equipped with a 150 W xenon lamp using an excitation wavelength of 332 nm and an emission wavelength of 454 nm. Quartz cells of 10 nm light path for excitation and 5 nm light path for emission were used. The time average was set at 10 s for each reading, and the machine response was 2 s. Increasing amounts of antimycin were added to the  $bc_1$  complex and incubated at room temperature for 2 min before measurement. Fluorescence by increasing amounts of antimycin in the absence of  $bc_1$  complex was measured as a control for each titration.

## RESULTS

**The Iron-Sulfur Protein Is Oriented in a *trans* Manner in the  $bc_1$  Dimer**—The yeast  $bc_1$  complex was recently crystallized, and its three-dimensional structure has been determined (17). The crystal structure showed that the yeast  $bc_1$  complex is a dimer, as was previously shown for the beef and the chicken enzymes (18–20). In the dimer the two copies of the Rieske iron-sulfur protein are intertwined and oriented in a *trans* manner with respect to each monomer as shown in Fig. 1A. The head domain of the iron-sulfur protein comes in close contact with heme  $b_L$  of cytochrome  $b$  and cytochrome  $c_1$  of one monomer, whereas the N-terminal and transmembrane domains of the protein are anchored in the other monomer, close to heme  $b_H$ . Confirmation of an intertwined dimer in solution was provided when a stable  $bc_1$  complex from *Rhodobacter sphaeroides* was generated carrying two intersubunit disulfide bonds, one between the head domain of the iron-sulfur protein and cytochrome  $b$  and the other between the tail domain of the iron-sulfur protein and cytochrome  $b$  (21).

The iron-sulfur protein molecule contains three domains, an extrinsic domain consisting of residues 93–215, a linker region consisting of residues 81–92, and a transmembrane domain consisting of residues 51–80. The extrinsic domain carries the iron-sulfur cluster and forms, together with a domain in cytochrome  $b$  proximal to heme  $b_L$ , the ubiquinol oxidizing pocket, center P (17, 20, 22). The transmembrane region of the iron-sulfur protein is an alpha helix, as shown in Fig. 1A. The tail of the transmembrane region comes within 20 Å of the quinone reducing center N. This is the region where ubiquinone closely interacts with heme  $b_H$  of cytochrome  $b$ , indicated by the arrow pointing to the ubiquinone head-group in Fig. 1A. The transmembrane domain of the iron-sulfur protein is in close contact with helix E of cytochrome  $b$ , which abuts heme  $b_H$  at center N.

Three layers of antiparallel  $\beta$ -strands surround the [2Fe-2S] cluster, which is coordinated by His-161, His-181, Cys-159, and Cys-178 as shown in Fig. 1B. A hydrogen bond network to the iron-sulfur cluster includes Ser-183 and Tyr-185, located in the  $\beta 7$  strand. These two residues are conserved in all Rieske iron-sulfur proteins that oxidize ubiquinol. The hydroxyl group of Ser-183 is hydrogen-bonded to S1 at a distance of 3.2 Å.

In a previous study (9) we characterized mutations in Ser-183 that altered the cytochrome  $c$  reductase activity of the  $bc_1$

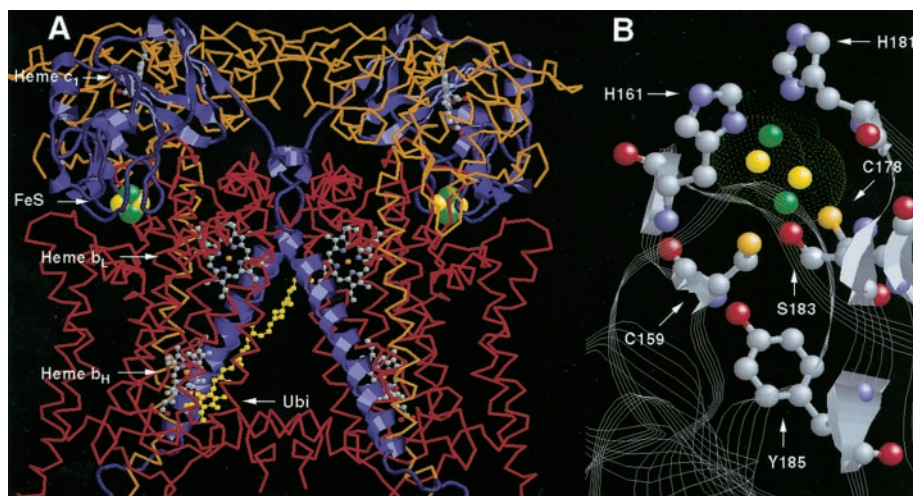


**FIG. 1. Structure of the Rieske iron-sulfur protein in the cytochrome  $bc_1$  complex and the iron-sulfur cluster environment.** The figure on the left shows the redox subunits of the cytochrome  $bc_1$  complex. The backbone structures of cytochrome  $b$  and cytochrome  $c_1$  are shown in red and orange, respectively, and the Rieske iron-sulfur protein is shown as a blue ribbon. The heme groups of cytochrome  $b$  (heme  $b_H$  and heme  $b_L$ ) and cytochrome  $c_1$  (heme  $c_1$ ) are depicted as ball and stick structures with CPK coloring. The iron-sulfur protein (FeS) is depicted as a space-filled model with the iron and sulfur atoms colored green and yellow, respectively. Ubiquinone (Ubi) is depicted as a yellow ball and stick structure. The figure was constructed from the coordinates of the yeast cytochrome  $bc_1$  complex (17), with the non-redox subunits omitted. The figure on the right shows an expanded view of the environment around the Rieske iron-sulfur cluster and is rotated 180° relative to the view on the left. The iron-sulfur cluster is depicted as balls surrounded by dots with the iron and sulfur atoms colored green and yellow, respectively. His-161, His-181, Cys-159, and Cys-178, which are ligands to the iron atoms of the cluster, are depicted as ball and stick structures with CPK coloring. Ser-183 and Tyr-185, which form hydrogen bonds to a sulfur atom in the cluster and to Cys-159, respectively, are also depicted as ball and stick structures with CPK coloring. The remainder of the Rieske protein is depicted as a strand.

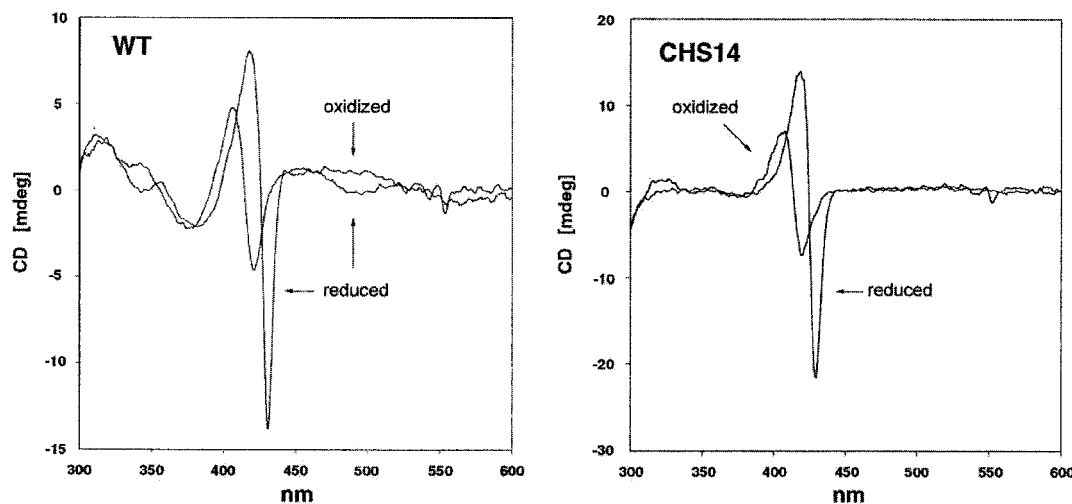


**FIG. 2. Circular dichroism spectra of purified cytochrome  $bc_1$  complexes from wild-type yeast and the CHS14 mutant.** The fully reduced spectra were taken at  $-413$  mV (wild-type) and  $-411$  mV (CHS14), and the fully oxidized spectra were taken at  $+487$  mV (wild-type) and  $+489$  mV (CHS14).

complex due to changes in the midpoint potential of the iron-sulfur protein. An S183T mutation that weakened the hydrogen bond from Ser-183 to the iron-sulfur cluster dropped the midpoint potential by 26 mV and caused a 20% loss of activity. An S183A mutation that eliminated the hydrogen bond dropped the midpoint potential of the iron-sulfur protein from  $+285$  mV to  $+150$  mV and caused a 90% loss of activity. We also noted that when Ser-183 was replaced with Cys the resulting yeast were petite and the mitochondrial membranes had no  $bc_1$  complex activity (6, 9). However, we did not investigate the basis for loss of  $bc_1$  complex activity. We thus proceeded to further characterize the  $bc_1$  complex from the respiratory-deficient yeast carrying the S183C mutation in the Rieske iron-sulfur protein.

**Insertion of Iron-Sulfur Protein Lacking the Iron-Sulfur Cluster into the Cytochrome  $bc_1$  Complex**—We first examined

the iron-sulfur cluster in the isolated  $bc_1$  complex from the CHS14 yeast mutant carrying the S183C mutation in the Rieske protein and compared it with that from a wild-type  $bc_1$  complex. In the reduced state the  $bc_1$  complex from wild-type yeast shows a negative CD band at 500 nm, which is free of interfering signals as shown in Fig. 2A. The  $bc_1$  complex from the CHS14 mutant lacks the 500 nm band (Fig. 2B), indicating that the cluster is absent and therefore explaining the absence of  $bc_1$  complex activity in the mutant (6, 9). Because the 500-nm CD band characteristic of the iron-sulfur cluster was not detectable, no attempt was made to characterize the cluster by EPR spectroscopy.

We previously observed that mutations in the highly conserved cysteines and histidines that ligate the cluster cause loss of the iron-sulfur cluster and very low amounts of the apoprotein present in the  $bc_1$  complexes from those mutants

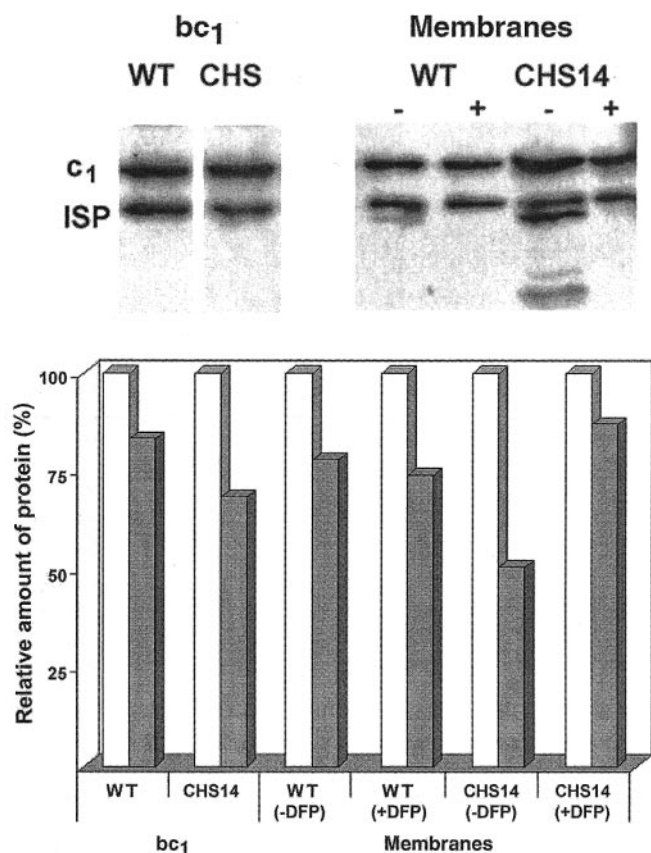


FIG. 3. Immunoblot analysis of iron-sulfur protein content in mitochondrial membranes and isolated  $bc_1$  complexes from wild-type yeast and the CHS14 mutant. Mitochondrial membranes and purified cytochrome  $bc_1$  complexes were isolated in the presence of DFP from yeast containing wild-type (WT) and mutant iron-sulfur protein (CHS14). To determine the protease susceptibility of the samples the membranes were diluted into SDS gel buffer in the absence or presence of DFP as indicated, resolved by SDS-PAGE, and analyzed by Western blot analysis as shown at the top of the figure, using monoclonal antibodies to the Rieske iron-sulfur protein and cytochrome  $c_1$ . The purified  $bc_1$  complex was treated in the same manner, but no difference was observed (results not shown). The relative amounts of iron-sulfur protein and cytochrome  $c_1$ , shown at the bottom of the figure, were determined by scanning the stained gel. The amount of cytochrome  $c_1$  in each sample, indicated by the open bars, was arbitrarily set at 100%, and the amount of mature size iron-sulfur protein relative to cytochrome  $c_1$  was calculated from the densitometry scan for the wild-type and mutant  $bc_1$  complexes and for the wild-type membranes.

(5). To check for loss of the iron-sulfur apoprotein from the  $bc_1$  complex in the CHS14 mutant, we performed a Western blot analysis to compare the amounts of apoprotein in mitochondrial membranes and isolated enzyme. The top panel in Fig. 3 shows the Western blot analysis of wild-type and CHS14 membranes and pure  $bc_1$  complexes, and the lower panel shows the quantification of the scans. The amount of cytochrome  $c_1$  in each sample was arbitrarily set at 100%, and the amount of iron-sulfur protein relative to cytochrome  $c_1$  was calculated from the densitometry scan. The amount of iron-sulfur protein relative to cytochrome  $c_1$  in the purified  $bc_1$  complex from the CHS14 mutant is 83% of that in the wild-type  $bc_1$  complex, if the enzyme is isolated in the presence of the protease inhibitor DFP (Fig. 3). This indicates that the apoprotein is assembled into both halves of the  $bc_1$  dimer but somewhat more readily lost from the enzyme if the iron-sulfur cluster is absent. Lack of iron-sulfur cluster does not affect processing of the protein to mature size by the mitochondrial processing peptidases because there is no accumulation of intermediate-ISP in the membranes or in the isolated enzyme from the CHS14 mutant.

This contrasts with mutants where amino acids in the presequence that are recognized by mitochondrial processing peptidases have been mutated (11).

Although the iron-sulfur protein is assembled into the  $bc_1$  complex and processed to mature size in the CHS14 mutant, it is more sensitive to proteolysis than the iron-sulfur protein in the membranes from the wild-type yeast if protease inhibitor is omitted. When membranes were isolated from the wild-type yeast without DFP there is a small, but detectable, amount of proteolysis of the iron-sulfur protein in the membranes (Fig. 3). Consequently, the amounts of iron-sulfur protein relative to cytochrome  $c_1$  in membranes isolated from the wild-type yeast in the presence or absence of DFP are essentially identical (+5%).

If DFP is omitted during isolation of mitochondrial membranes from the CHS14 mutant, there is extensive proteolysis of the iron-sulfur protein as shown by the appearance of proteolytic degradation products as lower molecular weight bands. Consequently, the amount of iron-sulfur protein in membranes from the CHS14 mutant is only 58% as much in the wild-type membranes. By a similar Western blot analysis we observed that the proteolytic degradation products were lost when the  $bc_1$  complex was purified from these membranes (results not shown).

As mentioned above, the residue mutated in the CHS14 mutant, Ser-183, has been changed to Thr, Ala, and Cys (9). The first two mutations caused a change in the iron-sulfur protein redox potential, but the protein remained in normal amounts and retained the cluster. It seems that the Ser-183 hydroxyl group is not essential for the formation of the cluster, as evidenced by the presence of the cluster in the S183A form of the protein. Although the S183C mutation caused the loss of the cluster, the apoprotein is stable if protected from proteolysis. Therefore, it appears that an additional Cys residue interferes with insertion of the [2Fe-2S] cluster, but it can stabilize the extrinsic domain and therefore the protein, possibly by forming a disulfide bridge with Cys-159 or Cys-178 in this region (see Fig. 1B). Modeling of the S183C mutation indicates that the sulfur of the introduced Cys-183 is 4.15 Å from the sulfur of Cys-159 and 3.16 Å from the sulfur of Cys-178.

*Failure to Insert the Iron-Sulfur Cluster Blocks Ubiquinol Oxidation and Additionally Impairs Assembly of Center P in the S183C Mutant*—Lack of the 500-nm signal in the CD spectrum of the mutant  $bc_1$  complex (Fig. 2) shows conclusively that the iron-sulfur cluster is lost, whereas the Western blots (Fig. 3) show that the apoprotein remains in the membranes and in the purified enzyme. We thus decided to further characterize center P and center N in the purified enzyme to understand what effects the S183C mutation has on the structure of the  $bc_1$  complex.

As expected, there was no reduction of cytochrome  $b$  or cytochrome  $c_1$  via center P due to the absence of the iron-sulfur cluster (results not shown). There is also a change in the structure of center P, as indicated by a change in binding of myxothiazol to the  $bc_1$  complex from the CHS14 mutant. Myxothiazol was shown to bind at center P of the bovine  $bc_1$  complex with a stoichiometry of one myxothiazol per  $bc_1$  monomer and to cause a red shift in the optical spectrum of cytochrome  $b_L$  (13, 23, 24). A binding stoichiometry of one myxothiazol per  $bc_1$  monomer was similarly demonstrated for the yeast  $bc_1$  complex by titrating the myxothiazol-induced shift in the cytochrome  $b$  optical spectrum (25).

We thus used the shift in the cytochrome  $b$  optical spectrum induced by myxothiazol binding to probe the structure of center P in the  $bc_1$  complex from the CHS14 mutant. As can be seen in Fig. 4, whereas a binding stoichiometry of one myxothiazol per

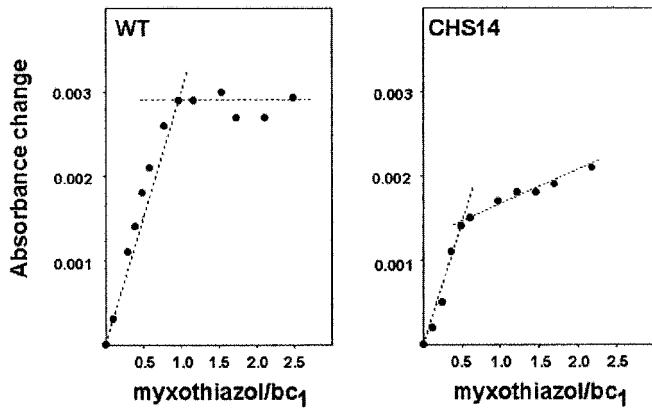


FIG. 4. Titration of the red shift in the cytochrome *b* spectrum caused by myxothiazol binding. Samples containing  $3.0 \mu\text{M}$   $bc_1$  complex from the wild-type (WT) yeast or the CHS14 mutant were reduced with dithionite and titrated with increasing amounts of myxothiazol. The increment of absorbance in the red shift caused by myxothiazol binding was plotted as a function of the ratio inhibitor: $bc_1$  complex. The dashed lines show theoretical titration curves assuming high affinity binding of 1.0 myxothiazol per  $bc_1$  complex for the wild-type enzyme and 0.5 myxothiazol per  $bc_1$  complex for the CHS14 enzyme, with a second, non-saturable binding site.

$bc_1$  monomer was observed with the enzyme from the wild-type yeast, the stoichiometry with the enzyme from the CHS14 mutant was only 0.5 per  $bc_1$  monomer. This result was unexpected because it has been shown that binding of similar methoxyacrylates is unaffected when the Rieske protein is extracted from the bovine  $bc_1$  complex (22). This suggests that failure to insert the iron-sulfur cluster alters the structure of center P.

**Improper Assembly of the Rieske Iron-Sulfur Protein Interferes with Assembly of Center N in the S183C Mutant**—To see if the S183C mutation had an effect on center N of the  $bc_1$  complex, we examined the rates of cytochrome *b* reduction through center N in the CHS14  $bc_1$  complex as a function of menaquinol concentration. As can be seen in Fig. 5, the second order rate constant for cytochrome *b* reduction in the wild-type  $bc_1$  complex decreased from  $5.3 \times 10^5 \text{ M}^{-1}\text{s}^{-1}$  to  $2.2 \times 10^5 \text{ M}^{-1}\text{s}^{-1}$  as the concentration of menaquinol increased. In the  $bc_1$  complex from the CHS14 mutant the second order rate constant decreased from  $5.4 \times 10^5 \text{ M}^{-1}\text{s}^{-1}$  to  $1.64 \times 10^5 \text{ M}^{-1}\text{s}^{-1}$ . From these results we conclude that the rate of electron transfer through center N is not significantly changed by the absence of iron-sulfur cluster. Although the rate constant is slightly smaller at higher menaquinol concentrations in the  $bc_1$  complex from the CHS14 mutant than in the wild-type enzyme, we consider this change insignificant in view of the limited number of data points.

Although the rate of cytochrome *b* reduction is the same in the  $bc_1$  complexes from the wild-type and CHS14 mutant, the amount of cytochrome *b* that is reducible through center N is significantly decreased in the mutant. Fig. 6 shows spectra of the  $bc_1$  complexes after reduction with  $25 \mu\text{M}$  menaquinol and dithionite. Stigmatellin was included with the wild-type  $bc_1$  complex to prevent reduction through center P in that enzyme. In the  $bc_1$  complex from the wild-type yeast menaquinol reduced 59% of the dithionite-reducible cytochrome *b*. In contrast, menaquinol reduced only 37% of the dithionite-reducible cytochrome *b* in the CHS14  $bc_1$  complex. This difference remained constant when using higher concentrations of menaquinol. For example, 61 and 41% of the dithionite-reducible cytochrome *b* were reduced with  $75 \mu\text{M}$  menaquinol in the wild-type and mutant  $bc_1$  complexes, respectively (data not shown). Notably, there is no damage to the cytochrome *b* in the

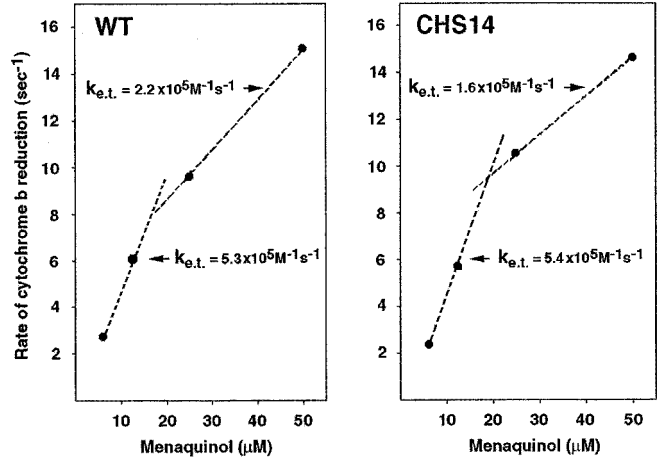


FIG. 5. Rates of cytochrome *b* reduction through center N in  $bc_1$  complexes from wild-type yeast and the CHS14 mutant. Pre-steady state rates of cytochrome *b* reduction were obtained by stopped flow rapid scanning spectroscopy (25) after reducing  $1.0 \mu\text{M}$  cytochrome  $bc_1$  complex with various concentrations of menaquinol as indicated in the figure legend. The rates of cytochrome *b* reduction in the  $bc_1$  complexes from the wild-type (WT) yeast and the CHS14 mutant are plotted as a function of menaquinol concentration. Dashed lines indicate the slopes used to calculate the second order rate constants.

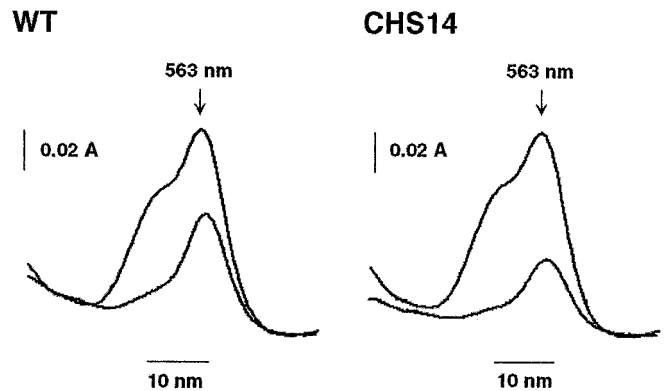


FIG. 6. Optical spectra of  $bc_1$  complexes from wild-type yeast and the CHS14 mutant after reduction with menaquinol or dithionite. Cytochrome  $bc_1$  complexes from the wild-type (WT) yeast and the CHS14 mutant were reduced with  $50 \mu\text{M}$  menaquinol. A 2-fold excess of stigmatellin was added to the wild-type enzyme to prevent reduction through center P. The enzymes were then reduced with dithionite. The lower trace shows the menaquinol-reduced minus oxidized spectra, and the upper trace shows the dithionite-reduced minus oxidized spectra for both  $bc_1$  complexes. Menaquinol reduced 59% of the dithionite-reduced cytochrome *b* in the wild-type  $bc_1$  complex, whereas the mutant cytochrome *b* was reduced only 37% with menaquinol.

CHS14 mutant  $bc_1$  complex. The spectrum of the dithionite-reduced  $bc_1$  complex shows the same absorption maximum and the same 2:1 ratio of  $b:c_1$  for the wild-type and mutant  $bc_1$  complexes.

To further characterize center N in the mutant, we titrated the pre-steady state reduction of cytochrome *b* with antimycin as described previously (14, 25). In this assay,  $bc_1$  complex was pre-mixed with antimycin and then reduced with  $25 \mu\text{M}$  menaquinol. To block reduction of cytochrome *b* through center P in the wild-type  $bc_1$  complex, the enzyme was mixed with stigmatellin. As shown in Fig. 7, reduction of cytochrome *b* through center N is inhibited by antimycin. With  $bc_1$  complex from wild-type yeast the stoichiometry is 1:1, but with the enzyme from the CHS14 mutant the stoichiometry is 0.5 antimycin per  $bc_1$  monomer.

Antimycin causes a red shift in the alpha band of the cytochrome *b* spectrum upon binding to reduced  $bc_1$  complex (13).

FIG. 7. Inhibition of the pre-steady state reduction of cytochrome  $b$  by antimycin in the isolated  $bc_1$  complexes from wild-type and CHS14 mutant. Cytochrome  $bc_1$  complexes were suspended at a concentration of  $1.5 \mu\text{M}$  and reduced with  $25 \mu\text{M}$  menaquinol. Prior to reduction the enzymes were pre-incubated with varying amounts of antimycin as indicated, and 2 equivalents of stigmatellin was pre-mixed with the wild-type enzyme to block reduction of cytochrome  $b$  through center P. The dashed lines show the linear fitting of 1.0 and 0.5 equivalents of antimycin per  $bc_1$  complex.

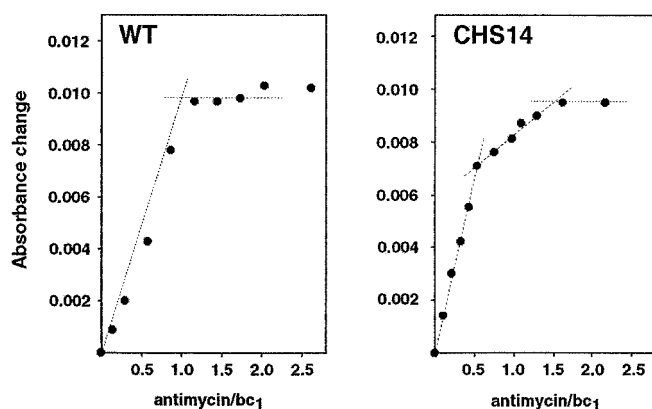
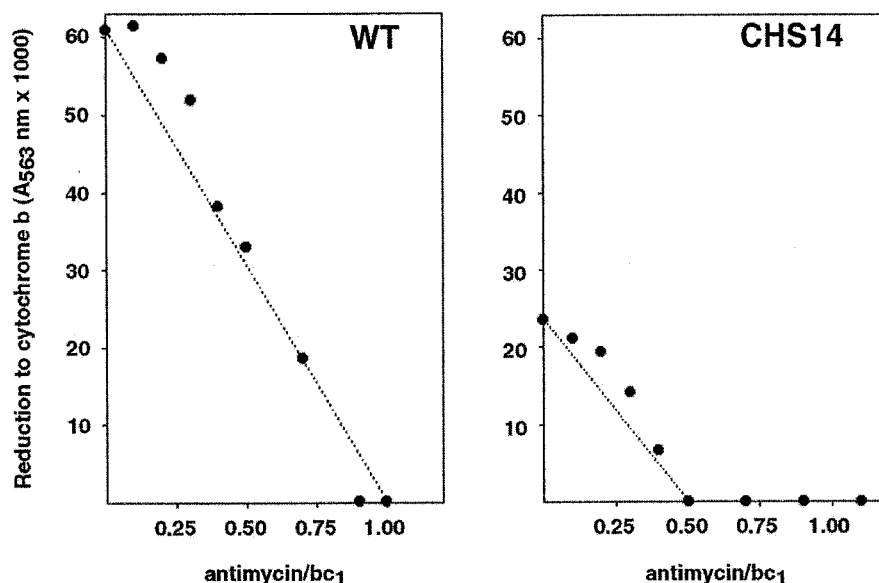


FIG. 8. Titration of the red shift in the cytochrome  $b$  spectrum caused by antimycin binding. Samples containing  $3.1 \mu\text{M}$   $bc_1$  complex from the wild-type (WT) yeast and  $3.4 \mu\text{M}$   $bc_1$  complex from the CHS14 mutant were reduced with dithionite and titrated with increasing amounts of antimycin. The absorbance increment resulting from the red shift in the absorbance spectrum caused by antimycin binding was plotted as a function of the ratio inhibitor: $bc_1$  complex. The dashed lines show fitted curves assuming high affinity binding of one inhibitor molecule per  $bc_1$  complex to the wild-type enzyme and binding of 0.5 inhibitor per  $bc_1$  complex with high affinity and non-stoichiometric binding of a second inhibitor molecule at a low affinity site in the mutant.

To further evaluate the titer for antimycin binding we titrated the antimycin-induced red shift in the spectrum of the CHS14  $bc_1$  complex and compared it the red shift of a wild-type  $bc_1$  complex as shown in Fig. 8. As antimycin is titrated into the wild-type  $bc_1$  complex the absorbance change increases until a stoichiometry of one antimycin per  $bc_1$  complex is obtained, after which there is very little absorbance change upon further additions of the inhibitor. In contrast, the titration of antimycin into the CHS14  $bc_1$  complex is biphasic. The absorbance increases incrementally until 0.5 equivalents of antimycin per  $bc_1$  complex are added, and then there is a more gradual increment in absorbance as additional antimycin is added. These results indicate that antimycin binds with equal affinity to both center N sites in the dimeric  $bc_1$  complex from the wild-type yeast but that it binds with significantly different affinities to the two sites in the  $bc_1$  complex from the CHS14 mutant.

We also used the quenching of antimycin fluorescence to

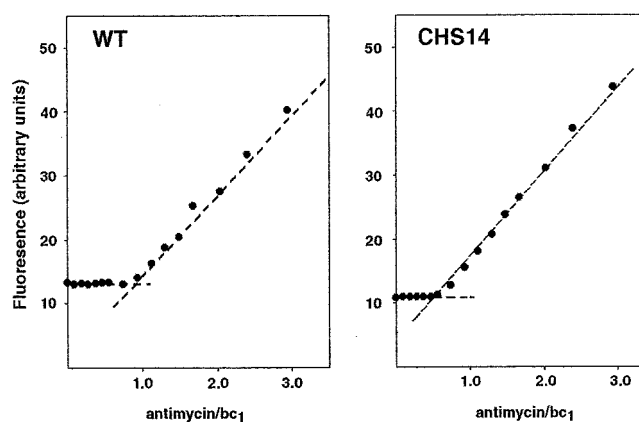


FIG. 9. Quenching of antimycin fluorescence by binding to isolated  $bc_1$  complexes. The fluorescence of a solution containing  $2.2 \mu\text{M}$  oxidized  $bc_1$  complex from the wild-type (WT) yeast or the CHS14 mutant in assay buffer (pH 7.0) was measured in the presence of increasing amounts of antimycin using an excitation wavelength of 332 nm and an emission wavelength of 454 nm.

examine the binding stoichiometry. Upon binding to the  $bc_1$  complex antimycin fluorescence is quenched, and when the enzyme becomes saturated further addition of antimycin results in incremental increases in fluorescence. This allows the binding to be measured under conditions where the  $b$  hemes are oxidized. As shown in Fig. 9, quenching of the antimycin fluorescence is saturated in the wild-type  $bc_1$  complex when the stoichiometry of binding reaches a value close to one equivalent of antimycin per  $bc_1$  monomer, in agreement with the results previously obtained by this method (16). The titer for quenching of antimycin fluorescence in the  $bc_1$  complex from the CHS14 mutant indicated a high affinity binding site that becomes saturated at 0.5 equivalents per  $bc_1$  complex, thus confirming the results from titration of the red shift in the optical spectrum. A second, lower affinity binding site is not obvious from the fluorescence quenching titration, but it is possible that it is not revealed in this titration due to the limited number of data points.

#### DISCUSSION

The striking finding from our results is that failure to insert the [2Fe-2S] cluster into the Rieske iron-sulfur affects the structure of center N, which is on the opposite side of the

membrane from the extrinsic domain where the cluster is located. Although the head domain of the Rieske protein and center N are located on opposite sides of the mitochondrial membrane, there is genetic evidence for interaction between these two sites. In *Rhodobacter capsulatus* a series of revertants were isolated from mutations at Leu-136 of the *Rhodobacter* iron-sulfur protein, equivalent to Ile-167 in the yeast protein, which is located within 8.5 Å of the iron-sulfur cluster in the head domain of the Rieske protein (26). Some of the revertants were compensatory mutations located on residues 44 or 46 of the N-terminal domain of the *Rhodobacter* protein, near center N. This indicates a structural interaction between the head domain of the Rieske protein and center N across the bacterial membrane. Single mutations generated on the latter two amino acids in the absence of the mutation on residue 136 were without phenotype as regards photosynthetic growth, inhibitor sensitivity, and EPR spectra, but the redox potential of the iron-sulfur cluster increased from 312 to 385 mV. This demonstrates that a structural change in the N-terminal domain of the Rieske protein can effect the properties of the iron-sulfur cluster.

By various criteria we found that 50% of the  $bc_1$  complex was damaged at center P and center N. Because the  $bc_1$  complex is a dimer this could indicate that 50% of the enzyme is damaged or that one monomer in all of the dimers is damaged. If the entire enzyme dimer were damaged, one would expect the extent of inactive enzyme to vary in multiple preparations. The fact that the titer for inhibitors was consistently diminished to one per dimer in multiple preparations of enzyme suggests that one monomer in all of the dimers is damaged.

The S183C mutation alters the binding of ligands at both centers P and N. The stoichiometry of myxothiazol binding in the  $bc_1$  complex from the mutant indicates that center P can bind only one inhibitor per dimer. Whereas deletion of the gene for the Rieske iron-sulfur protein causes a decrease in the alpha band of cytochrome *b* (27), the presence of a stable iron-sulfur protein without cluster does not have an effect on the spectrum of cytochrome *b*. This suggests that the structural change at center P is subtle and has not affected the heme  $b_L$  environment.

The structural change at center N is also subtle. Although the decreased reduction of cytochrome *b* by menaquinol through center N suggests that menaquinol reacts with only one half of the dimer and only one antimycin is bound with high affinity to the dimer, the optical spectrum indicates there was no significant change in the heme  $b_H$  environment.

The crystal structure of the  $bc_1$  complex shows that the iron-sulfur protein forms center P of one monomer and is close to center N in the second monomer. Because the iron-sulfur

protein is intertwined in the dimeric enzyme we hypothesize that a mutation in the extrinsic head domain of the iron-sulfur protein in one monomer exerts an effect across the membrane in a *trans* manner, affecting center N of the other monomer. The amounts of iron-sulfur protein in the purified enzyme from the CHS14 mutant indicate that the apoprotein is inserted into both halves of the dimer and remains during purification of the  $bc_1$  complex. The extent of protease susceptibility of the protein lacking the iron-sulfur cluster suggests that the protein is not properly inserted into one of the monomers. Taken together these results suggest that the S183C mutation allows the correct insertion of one iron-sulfur protein, but not the second, and only the correctly inserted iron-sulfur protein allows binding of ligands in each center.

## REFERENCES

- Hartl, F. U., Schmidt, B., Wachter, E., Weiss, H., and Neupert, W. (1986) *Cell* **47**, 939–951
- Brandt, U., Yu, L., Yu, C. A., and Trumpower, B. L. (1993) *J. Biol. Chem.* **268**, 8387–8390
- Nett, J. H., Schägger, H., and Trumpower, B. L. (1998) *J. Biol. Chem.* **273**, 8652–8658
- Nett, J. H., Denke, E., and Trumpower, B. L. (1997) *J. Biol. Chem.* **274**, 2212–2217
- Graham, L. A., and Trumpower, B. L. (1991) *J. Biol. Chem.* **266**, 22485–22492
- Nett, J. H., and Trumpower, B. L. (1999) *J. Biol. Chem.* **274**, 9253–9257
- Ljungdahl, P. O., Pennoyer, J. D., Robertson, D. E., and Trumpower, B. L. (1987) **891**, 227–241
- Snyder, C. H., and Trumpower, B. L. (1999) *J. Biol. Chem.* **274**, 31209–31216
- Denke, E., Merbitz-Zahradnik, T., Hatzfeld, O. M., Snyder, C., Link, T. A., and Trumpower, B. L. (1998) *J. Biol. Chem.* **273**, 9085–9093
- Link, T. A., Hatzfeld, O. M., Unalkat, P., Shergill, J. C., Cammack, R., and Mason, J. R. (1996) *Biochemistry* **35**, 7546–7552
- Laemmli, U. K. (1970) *Nature* **227**, 680–685
- Towbin, H., Staehelin, T., and Gordon, J. (1979) *Proc. Natl. Acad. Sci. U. S. A.* **76**, 4350–4354
- von Jagow, G., and Link, T. A. (1986) *Methods Enzymol.* **126**, 253–271
- Snyder, C. H., and Trumpower, B. L. (1998) *Biochim. Biophys. Acta.* **1365**, 125–134
- Cavazzoni, M., Svobodova, J., Desantis, A., Fato, R., and Lenaz, G. (1993) *Arch. Biochem. Biophys.* **303**, 246–254
- Berden, J. A., and Slater, E. C. (1972) *Biochim. Biophys. Acta* **256**, 199–215
- Hunte, C., Koepke, J., Lange, C., Rossmanith, T., and Michel, H. (2000) *Structure*, **8**, 669–684
- Xia, D., Yu, C. A., Kim, H., Xia, J. Z., Kachurin, A. M., Zhang, L., Yu, L., and Deisenhofer, J. (1997) *Science*. **277**, 60–66
- Iwata, S., Lee, J. W., Okada, K., Lee, J. K., Iwata, M., Rasmussen, B., Link, T. A., Ramaswamy, S., Jap, B. K. (1998) *Science*. **281**, 64–71
- Zhang, Z., Huang, L., Schulmeister, V. M., Chi, Y.-I., Kim, K.-K., Hung, L.-W., Crofts, A. R., Berry, E. A., and Kim, S.-H. (1998) *Nature*. **392**, 677–684
- Xiao, K., Chandrasekaran, A., Yu, L., and Yu C.-A. (2001) *J. Biol. Chem.* **276**, 46125–46131
- Brandt, U., Haase, U., Shägger, H., and von Jagow, G. (1991) *J. Biol. Chem.* **266**, 19958–19964
- von Jagow, G., and Engel, W. D. (1981) *FEBS Letts.* **136**, 19–24
- von Jagow, G., Ljungdahl, P. O., Graf, P., Ohnishi, T., and Trumpower, B. L. (1984) *J. Biol. Chem.* **259**, 6318–6326
- Gutierrez-Cirlos, E. B., and Trumpower, B. L. (2002) *J. Biol. Chem.* **277**, 1195–1202
- Brasseur, G., Sled, V., Liebl, U., Ohnishi, T., and Daldal, F. (1997) *Biochemistry*. **36**, 11685–11696
- Ljungdahl, P. O., Beckmann, J. D., and Trumpower, B. L. (1989) *J. Biol. Chem.* **264**, 3723–3731